Kyle L. Brown,[1] Carl Darris,[1] Kristie Lindsey Rose,[2] Otto A. Sanchez,[3] Hartman Madu,[1] Josh Avance,[4] Nickolas Brooks,[5] Ming-Zhi Zhang,[1] Agnes Fogo,[6] Raymond Harris,[1] Billy G. Hudson,[1,2,6] and Paul Voziyan[1]

Hypohalous Acids Contribute to Renal Extracellular Matrix Damage in Experimental Diabetes

Diabetes 2015;64:2242–2253 | DOI: 10.2337/db14-1001

In diabetes, toxic oxidative pathways are triggered by persistent hyperglycemia and contribute to diabetes complications. A major proposed pathogenic mechanism is the accumulation of protein modifications that are called advanced glycation end products. However, other nonenzymatic post-translational modifications may also contribute to pathogenic protein damage in diabetes. We demonstrate that hypohalous acid–derived modifications of renal tissues and extracellular matrix (ECM) proteins are significantly elevated in experimental diabetic nephropathy. Moreover, diabetic renal ECM shows diminished binding of α1β1 integrin consistent with the modification of collagen IV by hypochlorous (HOCl) and hypobromous acids. Noncollagenous (NC1) hexamers, key connection modules of collagen IV networks, are modified via oxidation and chlorination of tryptophan and bromination of tyrosine residues. Chlorotryptophan, a relatively minor modification, has not been previously found in proteins. In the NC1 hexamers isolated from diabetic kidneys, levels of HOCl-derived oxidized and chlorinated tryptophan residues W^{28} and W^{192} are significantly elevated compared with nondiabetic controls. Molecular dynamics simulations predicted a more relaxed NC1 hexamer tertiary structure and diminished assembly competence in diabetes; this was confirmed using limited proteolysis and denaturation/refolding. Our results suggest that hypohalous acid–derived modifications of renal ECM, and specifically collagen IV networks, contribute to functional protein damage in diabetes.

With an estimated half-billion people affected by the end of next decade, diabetes has become a pandemic. Diabetes complications such as nephropathy are of great concern as the life-threatening long-term consequences of persistent hyperglycemia. There is a pressing need for a better understanding of pathogenic mechanisms of diabetes complications to support rational development of novel therapeutic treatments.

Among the proposed mechanisms of diabetes complications is the activation of oxidative and glycoxidative pathways that cause pathogenic post-translational modifications of proteins, thus promoting organ dysfunction (1). Growing experimental evidence suggests that one of these pathways may involve hypohalous acids. Hypohalous acids are produced by a family of peroxidase enzymes, most prominently myeloperoxidase (MPO) and VPO-1/peroxidasin (2,3). MPO is a critical part of the innate immunity, while peroxidasin catalyzes reinforcement of collagen IV networks with sulfilimine cross-links (3). However, in the disease states, the overproduction of hypohalous acids by these enzymes may have pathogenic consequences. Indeed, the activation of MPO and the overproduction of hypochlorous acid (HOCl) have been reported in diabetes (4), and peroxidasin has been shown

[1]Department of Medicine, Vanderbilt University Medical Center, Nashville, TN
[2]Department of Biochemistry, Vanderbilt University Medical Center, Nashville, TN
[3]Institute of Imaging Science, Vanderbilt University Medical Center, Nashville, TN
[4]Berea College, Berea, KY
[5]Yale University, New Haven, CT
[6]Department of Pathology, Microbiology, and Immunology, Vanderbilt University Medical Center, Nashville, TN

Corresponding author: Paul Voziyan, paul.voziyan@vanderbilt.edu.

Received 27 June 2014 and accepted 10 January 2015.

This article contains Supplementary Data online at http://diabetes.diabetesjournals.org/lookup/suppl/doi:10.2337/db14-1001/-/DC1.

K.L.B. and C.D. contributed equally to this study.

O.A.S. is currently affiliated with the Epidemiology Clinical Research Center, University of Minnesota, Minneapolis, MN.

H.M. is currently affiliated with Meharry Medical College, Nashville, TN.

See accompanying article, p. 1910.

to mediate oxidative vascular damage and renal fibrosis (5–8). Other hypohalous acids and peroxidase enzymes may also be involved inasmuch as MPO, peroxidasin, and eosinophil peroxidase can produce hypobromous acid (HOBr) under physiological bromine concentrations and can cause protein bromination in vitro (9–11).

Several studies indicate that HOCl can modify proteins in vivo. An increase in HOCl-derived protein oxidation has been reported (2,12) in renal tissues of patients with chronic kidney disease. Also, MPO-derived HOCl has been shown to damage HDL, and to uncouple and inhibit endothelial nitric oxide synthase in atherosclerotic lesions (13–15). Both peroxidasin and MPO can bind to extracellular matrix (ECM) and, thus, may be particularly important in potential pathogenic modification of ECM proteins (3,8,16). The above reports from the literature imply that hypohalous acid–derived modifications may potentially accumulate in diabetic tissues, particularly in long-lived ECM proteins, which are the most susceptible to oxidative damage. However, the experimental evidence is absent. We set out to determine the sites of protein halogenation and its impact on ECM functionality in diabetes using preparations of renal ECM and noncollagenous (NC1) hexamers, which are critical connection modules of collagen IV networks (17).

We demonstrated that hypohalous acid–derived modifications of renal proteins are significantly elevated in experimental diabetic nephropathy models. Moreover, diabetic renal ECM showed diminished binding of α1β1 integrin that was consistent with modification of collagen IV by HOCl and HOBr. In diabetes, specific HOCl-derived oxotryptophan and chlorotryptophan residues of NC1 hexamers within collagen IV networks were significantly elevated compared with those from nondiabetic controls, causing more relaxed NC1 hexamer tertiary structure and diminished assembly competence. Our results suggest that hypohalous acid–derived modification of renal ECM can contribute to functional damage of collagen IV networks in diabetes.

RESEARCH DESIGN AND METHODS

Materials

Mouse collagen IV, guanidinium hydrochloride, proteinase K, and sodium hypochlorite solution were from Sigma-Aldrich. Purified human integrin α1β1 was from Millipore; and integrin β1 antibody was from Santa Cruz Biotechnology. DiBrY antibody was from Cosmo Bio USA (Carlsbad, CA).

Human Renal Tissues

Kidney samples (baseline donor biopsy samples or uninvolved tissue from tumor nephrectomies) were identified from our archival files. Diagnoses from biopsy samples were made after light microscopic, immunofluorescence, and electron microscopic examination. Studies of archival biopsy samples were approved by the Vanderbilt Institutional Review Board.

Animal Experiments

The principles of laboratory animal care were followed according to institutional animal care and use committee guidelines. A spontaneously diabetic eNOS$^{-/-}$ C57BLKS *db/db* mouse model of diabetic nephropathy, which recapitulates renal lesions found in human diabetic nephropathy, was produced and genotyped in-house (18,19). Diabetes was confirmed by measurement of glucose levels in blood collected from the tail vein, as previously described (18,19) (Table 1). The control group included age-matched wild-type C57BLKS mice. Animals were killed at 22 weeks of age. Kidneys were removed, fixed or flash frozen, and stored for further analyses.

Diabetes was induced in 10-week-old male Sprague-Dawley rats with intravenous administration of streptozotocin (STZ) (60 mg/kg); control rats were injected with saline solution. Blood glucose levels were measured two times per week using the glucose oxidase method. Animals were considered diabetic when glucose levels were at least 250 mg/dL. Diabetes was confirmed after 12 weeks by determining the plasma levels of glycated hemoglobin (Table 1). Kidneys were removed postmortem, fixed or flash frozen, and stored for further analyses.

Immunohistochemical detection of halogenated proteins in human, mouse, and rat renal sections was performed using an anti-DiBrY antibody, which recognizes brominated and chlorinated proteins (20). As a negative control, the primary antibody was omitted, and only the secondary antibody was used. For human tissue sections, antigen retrieval was performed in boiling 100 mmol/L citric acid buffer for 15 min. Kidney sections were incubated using the avidin-biotin-horseradish peroxidase technique (Elite Vectastain ABC kit; Vector Laboratories), and staining was visualized using 3,3′-diaminobenzidine. Quantitative image analysis was performed using the BIOQUANT Image Analysis software, as previously described (21).

Table 1—Hyperglycemia in STZ-induced rat and eNOS$^{-/-}$ C57BLKS mouse models of diabetes

	HbA_{1c}, % (mmol/mol)	Fasting blood glucose, mg/dL
STZ-induced rats		
Control	3.2 ± 0.1 (11.0 ± 1.1)	
Diabetic	7.6 ± 0.5 (60.0 ± 5.5)*	
eNOS$^{-/-}$ C57BLKS mice		
Control		115 ± 5
Diabetic		493 ± 82*

HbA_{1c} in rat plasma was measured after 12 weeks of diabetes using an automated analyzer based on ion exchange high-performance liquid chromatography technology. Fasting blood glucose was measured in mice after 16 weeks of diabetes using the glucose oxidase method. *$P < 0.01$, diabetic vs. control ($n = 8$).

Isolation and Analysis of Collagen IV NC1 Hexamers

Collagen IV NC1 hexamers were isolated from rat kidneys as previously described (22). For refolding/assembly studies, NC1 hexamers from control and STZ-induced diabetic rats were incubated in 50 mmol/L Tris acetate buffer, pH 7.4, with 6 mol/L GdnCl at 80°C for 30 min, followed by analysis using a Superdex 200 gel-filtration column equilibrated with the same buffer and AKTApurifier fast-protein liquid chromatography (FPLC) system.

For limited proteolysis studies, NC1 hexamers (1 mg/mL) were incubated in 50 mmol/L Tris-buffered saline solution (TBS), pH 7.5, alone or with 0.2 mmol/L HOCl for 2 h at 37°C. Samples were washed and digested at 50°C for 30 min with proteinase K (5:1, weight for weight) in 50 mmol/L Tris-HCl, pH 8.0, and 1 mmol/L dithiothreitol. Upon addition of the denaturing loading buffer containing 100 mmol/L dithiothreitol and heating at 90°C for 30 min, samples (8 μg of protein) were fractionated on 12% SDS-PAGE gels followed by Coomassie staining.

Decellularization and Homogenization of Mouse Kidney Samples

Kidney samples were placed in 1% SDS and incubated in a rotary mixer at 4°C for 5 days, with fresh solution changes every 24 h. A kidney sample (5 mg) was homogenized using a glass homogenizer in 300 μL of ice-cold 200 mmol/L sodium phosphate buffer, pH 7.5, supplemented with protease inhibitor cocktail.

Modification of Renal ECM and Collagen IV and Integrin Binding Assay

An aliquot (20 μg/mL) of either decellularized homogenized renal ECM or purified type IV collagen was immobilized on 96-well plates at 4°C overnight. Wells were washed with 100 mmol/L sodium phosphate buffer, pH 7.5, before being incubated in the same sodium phosphate buffer with either HOCl or HOBr. Incubations were carried out for 2 h at 37°C, and wells were washed with TBS. The binding of purified α1β1 integrin was determined using a solid-phase binding assay (23). The microplate well coating efficiency by collagen IV was >99% and was not affected by hypohalous acid treatment, as determined using an alkaline phosphatase competition assay (24).

Liquid Chromatography–Tandem Mass Spectrometry Analysis of Site-Specific Modifications in NC1 Domains of Collagen IV

The site-specific modifications in purified NC1 domains of collagen IV from rat kidneys were analyzed by liquid chromatography–tandem mass spectrometry (LC-MS/MS). Samples were precipitated with trichloroacetic acid, reduced with tris(2-carboxyethyl)phosphine, and alkylated with iodoacetamide. Tryptic digests were performed overnight at 37°C. Peptides were loaded onto a capillary column (360 μm outer diameter × 100 μm inner diameter) packed with C18 reverse-phase material (Jupiter, 3 μm beads, 300 Å; Phenomenex) and eluted at a flow rate of 500 nL/min. The mobile phase consisted of 0.1% formic acid in water (solvent A) and 0.1% formic acid in acetonitrile (solvent B). A 90-min gradient occurred as follows: 0–15 min, 2% solvent B (loading phase); 15–55 min, 2–40% solvent B; 55–65 min, 40–90% solvent B; 65–68 min, 90% solvent B; 68–70 min, 90–2% solvent B; and 70–90 min, 2% solvent B. Peptides were mass analyzed on a LTQ Orbitrap Velos mass spectrometer equipped with a nanoelectrospray ionization source. Database searches were performed using SEQUEST (25), and results were assembled in Scaffold version 3.6.4 with minimum filtering criteria of 95% peptide probability. Searches were configured to use variable protein residue modifications, as follows: carbamidomethylation on cysteine (ΔM = 57.0215); oxidation of methionine and histidine (ΔM = 15.9949); mono- and double chlorination of lysine, histidine, tyrosine, and tryptophan (ΔM = 33.9611 and 67.9222); mono- and double bromination of lysine, histidine, tyrosine, and tryptophan (ΔM = 77.9105 and 155.8210); singly and doubly oxidized tryptophan (ΔM = 15.9949 and 31.9898); nitrated tyrosine (ΔM = 44.9851); singly and doubly chlorinated phenylalanine (ΔM = 33.9611 and 67.9222); and hydroxylated lysine and proline (ΔM = 15.9949). All sites of modification were validated by manual interpretation of the raw tandem mass spectra using Xcalibur version 2.1.0 software. A window of 10 parts per million around the theoretical monoisotopic charge/mass ratio values of the observed precursor ions was used to generate extracted ion chromatograms. The integrated area under the curve for each extracted ion chromatogram peak was determined, and the relative abundance of each modified peptide was calculated as a percentage of the summed area under the curve obtained for all modified and unmodified peptide forms.

Molecular Dynamics Simulations

Molecular dynamics (MD) simulations used the AMBER 12 program suite and the ff99SB parameter set, as previously described (26). Starting coordinates were taken from the X-ray structure of bovine placenta collagen IV NC1 hexamer (PDB 1T61). The following three MD systems were constructed for comparative analyses: the wild-type NC1 $(\alpha1,\alpha1,\alpha2)_2$ hexamer; the NC1 $(\alpha1,\alpha1,\alpha2)_2$ hexamer, where W^{192} of the α1 chains and W^{28} of the α2 chains were chlorinated at carbon 7; and the NC1 $(\alpha1,\alpha1,\alpha2)_2$ hexamer with W^{192} of the α1 chains and W^{28} of the α2 chains oxidized at carbon 2 of the imidazole ring. Monovalent ion parameter sets were used as described previously (27), while divalent ion parameters were generated with the program xLEaP to model potassium and calcium ions native to the NC1 $(\alpha1,\alpha1,\alpha2)_2$ hexamer structure. MD systems were solvated in a truncated octahedral box using the TIP3P water model to a distance of 8.0 Å. Production calculations were conducted at constant pressure for 50 ns. Temperature was maintained at 300° Kelvin by a Langevin coupling algorithm using a collision frequency of 0.5 ps^{-1} (28).

Electrostatic interactions were treated with the particle mesh Ewald method (29). The program PyMOL (30) was used for molecular modeling and the interpretation of MD results.

Statistical Analyses

Statistical analysis was performed using one-way ANOVA followed by a post hoc Tukey test (SigmaStat version 4.0). Differences were considered statistically significant if P values were <0.05.

RESULTS

Halogenation of Renal Tissues in Experimental Diabetes

Animal renal sections were analyzed using immunohistochemical detection and an antibody that recognizes brominated and chlorinated proteins. We detected a significant increase in the levels of halogenated proteins in the renal glomerular and tubular regions in type 2 diabetic nephropathy and type 1 diabetic animal models compared with the corresponding nondiabetic controls (Fig. 1*A* and *B*).

Effect of ECM and Collagen IV Halogenation on Integrin Binding

Halogenation may have pathogenic significance only if it impacts protein function. Interaction with renal cells via integrin receptors is one of the key functions of renal ECM. We determined whether ECM halogenation can affect its interaction with integrin α1β1, the main physiological receptor for collagen IV. Significant inhibition of α1β1 integrin binding was detected in ECM preparations isolated from diabetic versus control mouse kidneys (Fig. 2*A*). To confirm that ECM halogenation can contribute to the inhibition of α1β1 integrin binding, renal ECM preparations from control mice were treated with either HOCl or HOBr. The binding of α1β1 integrin to these hypohalous acid–modified ECM specimens was significantly inhibited compared with unmodified ECM specimens (Fig. 2*B* and *C*). Moreover, the binding of α1β1 integrin to collagen IV was also inhibited upon modification of collagen IV with either HOCl or HOBr (Fig. 2*D* and *E*).

Oxidation and Halogenation of NC1 Hexamer of Collagen IV in Experimental Diabetes

To further assess sites of collagen IV halogenation in diabetes and the potential functional impact, we focused on its COOH-terminal NC1 domains, which encode the specificity of collagen IV network assembly in basement membranes (17). Within the networks, NC1 domains form hexameric connection modules that are stabilized via noncovalent interactions and sulfilamine bonds (31). To determine whether this critical network connection module can be damaged in diabetes via halogenation, we used an STZ-induced diabetic rat model. Preparations of

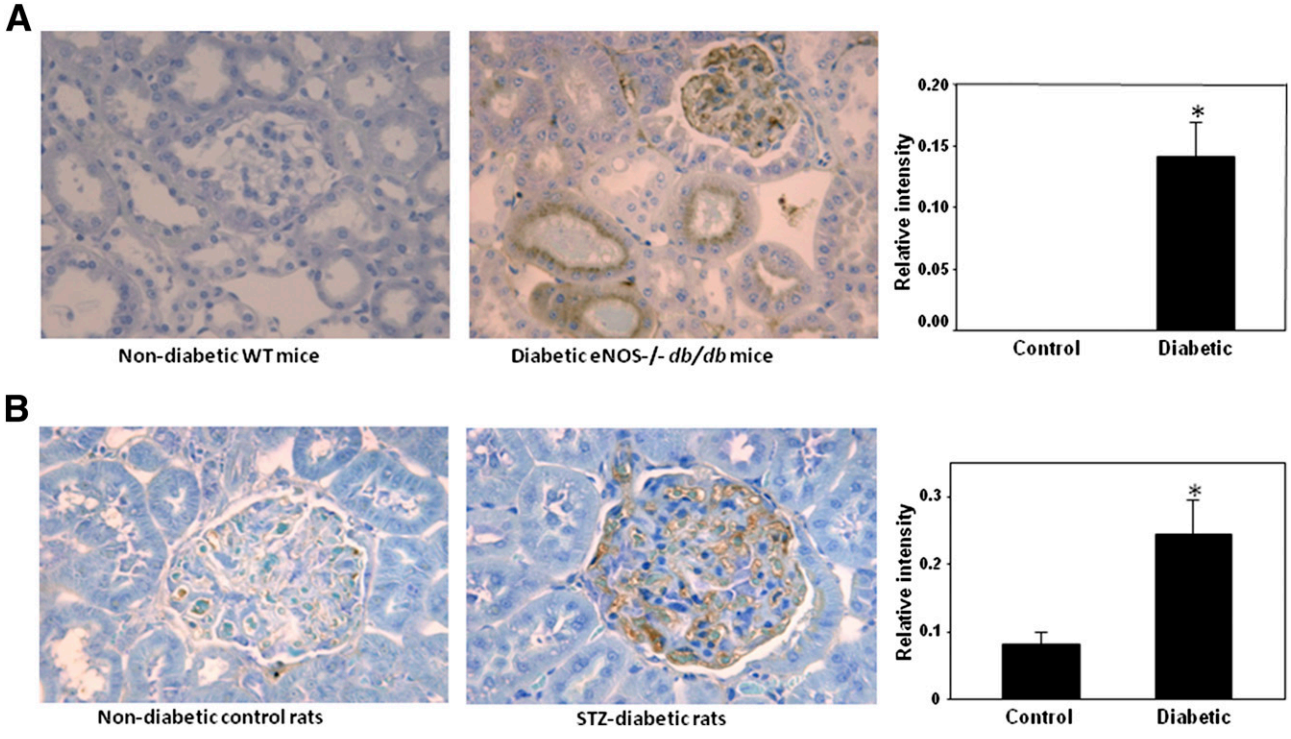

Figure 1—Detection of renal halogenated proteins in experimental diabetes. Renal sections from C57BLKS and eNOS$^{-/-}$ C57BLKS *db*/*db* mice (*A*) and from Sprague-Dawley control and STZ-induced diabetic rats (*B*) were analyzed using monoclonal antibody, which recognizes HOCl- and HOBr-modified proteins, as described in RESEARCH DESIGN AND METHODS. *$P < 0.01$, mouse/rat diabetic vs. control ($n = 5$). WT, wild type.

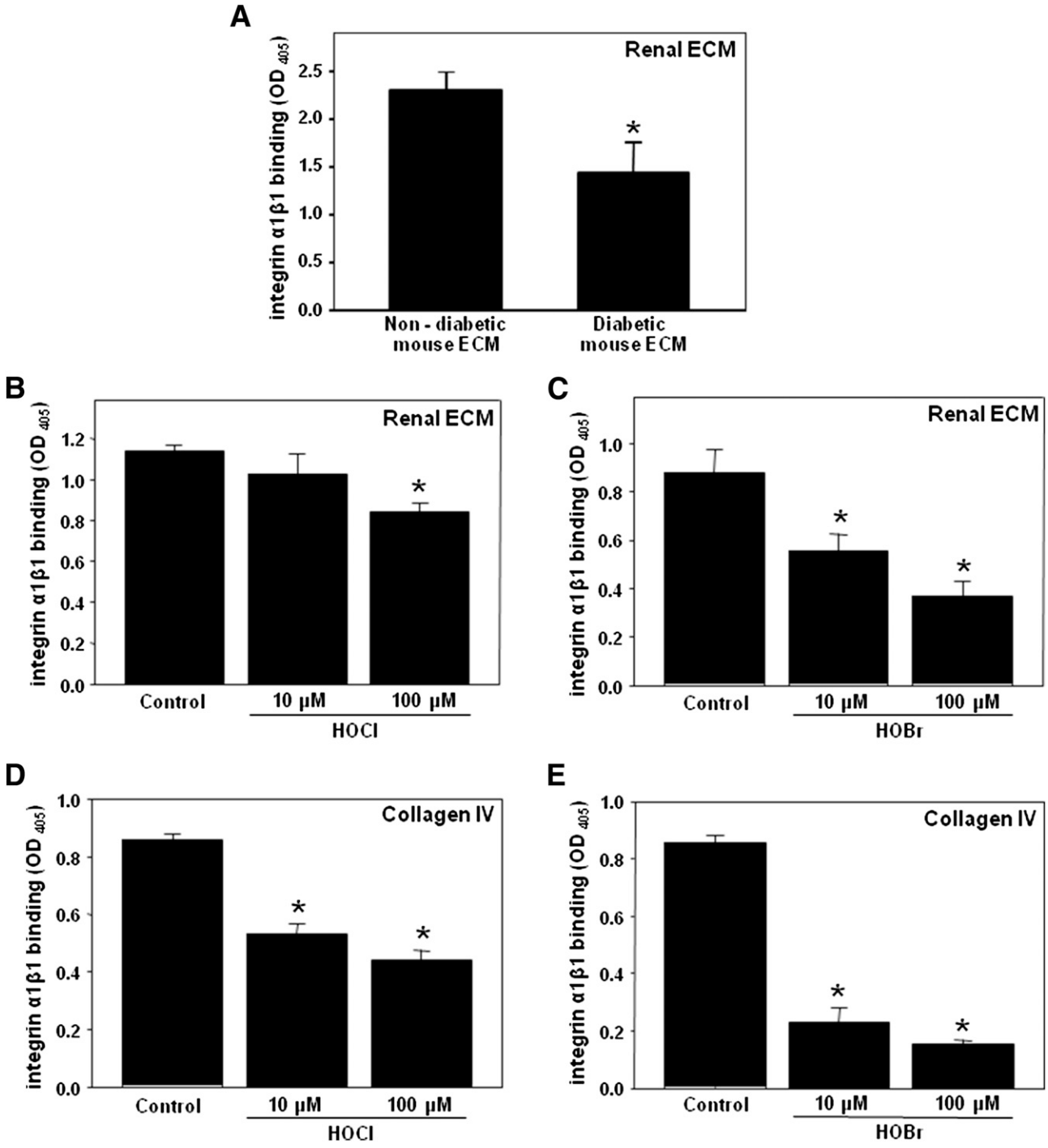

Figure 2—Binding of integrin $\alpha1\beta1$ to diabetic renal ECM, hypohalous acid–modified renal ECM, and hypohalous acid–modified collagen IV. *A*: Kidneys from C57BLKS (nondiabetic control) and $eNOS^{-/-}$ C57BLKS *db/db* (diabetic) mice were decellularized and homogenized as described in RESEARCH DESIGN AND METHODS. The binding of integrin $\alpha1\beta1$ to renal ECM homogenate was determined using a solid-phase binding assay. The bars represent background-subtracted Mn^{2+}-dependent binding. Each bar represents the mean ± SEM. **P* < 0.05, control vs. diabetic (*n* = 5). ECM homogenate from C57BLKS mice was coated onto 96-well plates and incubated with the indicated concentrations of either HOCl (*B*) or HOBr (*C*) for 2 h at 37°C. The binding of integrin $\alpha1\beta1$ to modified and unmodified renal ECM was determined as in *A*. **P* < 0.05, control vs. halogenated proteins (*n* = 4). Purified EHS collagen IV was coated onto 96-well plates and incubated with the indicated concentrations of either HOCl (*D*) or HOBr (*E*) for 2 h at 37°C. The binding of integrin $\alpha1\beta1$ to modified and unmodified collagen IV was determined as in *A*. **P* < 0.05, control vs. halogenated proteins (*n* = 4). OD, optical density.

NC1 hexamers isolated from renal ECM of control and diabetic animals were analyzed using LC-MS/MS for the presence of post-translational oxidative modifications associated with diabetes. We identified several oxidative modifications at specific tryptophan and tyrosine residues, including oxidation, chlorination, bromination, and nitration (Supplementary Tables 1 and 2 and Fig. 3). In diabetes, there was a significant twofold to fivefold increase in the levels of either oxidized or chlorinated W^{192} of α1NC1 domains and W^{28} of α2NC1 domains compared with nondiabetic controls (Table 2). Similar increases in the levels of these modifications in α3NC1 and α4NC1 domains were detected at the same sites (Supplementary Table 1). Levels of nitrated residues Y^{184}, Y^{185}, and Y^{189} within α1NC1 domain and a brominated residue Y^{6} within α2NC1 domain did not change in diabetic animals compared with controls (data not shown). No modifications were found on other NC1 domain residues with potential reactivity toward hypohalous acids (Fig. 3). The degree of oxidation of methionine residues, a known artifact of sample handling (32), was similar in NC1 domains isolated from diabetic and control animals (Supplementary Table 3). Thus, in NC1 domains isolated from rat kidneys, diabetes was associated with an increase in oxidation and chlorination of W^{28} and W^{192} residues. These modifications can potentially derive from reactions of tryptophan side chain with HOCl.

While HOCl-derived tryptophan oxidation has been demonstrated in vitro (33), chlorinated tryptophan residues have not previously been found in proteins. Since chlorotryptophan is a novel in vivo post-translational modification of proteins, we acquired more evidence from multiple experiments of the presence of this modification in rat NC1 domains, as follows: masses of chlorinated NC1 peptides were determined with high accuracy, within <1 part per million of theoretical masses (Supplementary Table 1); experimental isotopic envelopes of modified peptides matched theoretical isotopic envelopes and were consistent with the presence of chlorine atoms (Supplementary Fig. 1); MS^2 spectra of modified peptides showed characteristic peak shifts of 34 atomic mass units, consistent with chlorination of a specific tryptophan residue (Supplementary Fig. 2); and high-resolution MS^2 spectra demonstrated that the value of peak shifts matched the atomic mass of chlorine and that isotopic envelopes of modified but not unmodified peptide fragment ions were consistent with the presence of chlorine atoms (Supplementary Fig. 3).

Halogenation in Human Kidney

Using LC-MS/MS, we also found chlorinated tryptophan residue in NC1 hexamers isolated from nondiabetic human kidneys (Supplementary Fig. 4*A–D*). The presence of halogenated proteins in human kidneys was further confirmed by immunohistochemistry. Unlike in the animal kidney, the specific staining was localized to tubular regions with no visible glomerular staining (Supplementary Fig. 4*E*).

Oxidation and Chlorination of Specific Tryptophan Residues in NC1 Hexamer of Collagen IV Treated With HOCl

Detection of chlorinated tryptophan residues in NC1 hexamers pointed to HOCl as a potential source of this modification. Tryptophan oxidation is also consistent with HOCl action, as has been previously shown in in vitro experiments using model proteins (33). To determine

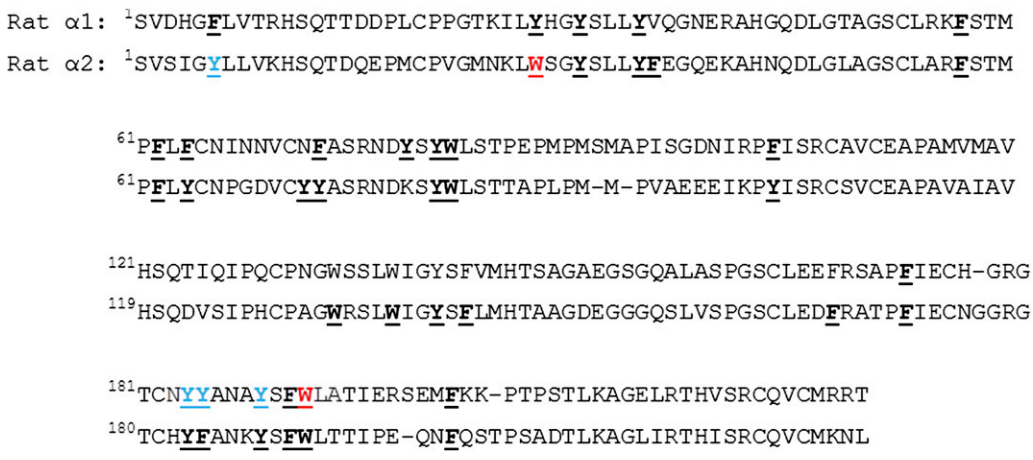

Figure 3—Location of oxidative modifications within primary structures of α1 (top sequence) and α2 (bottom sequence) domains of NC1 $(\alpha1,\alpha1,\alpha2)_2$ hexamer isolated from rat kidney collagen IV networks. A significant increase in the levels of oxidation and chlorination was detected in residues W^{192} (α1) and W^{28} (α2) of NC1 domains from diabetic rat kidneys compared with controls (shown in red). Brominated residue Y^{6} (α2) and nitrated residues Y^{184} (α1), Y^{185} (α1), and Y^{189} (α1) were also detected, but their levels were not changed in diabetic vs. control animals (shown in blue). Other aromatic residues susceptible to stable oxidation and/or halogenation were not modified (shown in bold black). Carbamidomethylated cysteine residues, oxidized methionine residues, and enzymatic PTMs hydroxylysine and hydroxyproline are not shown.

Table 2—Quantitation of modified tryptic peptides of α1 and α2 NC1 domains of collagen IV isolated from kidneys of control and STZ-induced diabetic rats

Peptide sequence	Normalized relative abundance, %		Fold change relative to control	Modified residue and Col IV chain
	Control	Diabetic		
(R^{179})GTC^{CAM}NYYANAYSF**W^{Cl}**LATIER(S^{199})	0.15 ± 0.02	0.77 ± 0.04*	5.13	W^{192} (α1)
(R^{179})GTC^{CAM}NYYANAYSF**W^{OH}**LATIER(S^{199})	10.62 ± 0.89	20.69 ± 0.82*	1.95	W^{192} (α1)
(K^{26})L**W^{Cl}**SGYSLLYFEGQEK(A^{42})	0.21 ± 0.04	1.08 ± 0.03*	5.14	W^{28} (α2)
(K^{26})L**W^{OH}**SGYSLLYFEGQEK(A^{42})	2.96 ± 0.27	9.97 ± 0.47*	3.37	W^{28} (α2)
(K^{26})L**W^{NFK}**SGYSLLYFEGQEK(A^{42})	4.77 ± 0.34	9.23 ± 0.59*	1.94	W^{28} (α2)

CAM, carbamidomethylation; Cl, chlorination; NFK, N-formyl kynurenine (or dihydroxytryptophan); Normalized relative abundance, (modified peptide/all forms of modified peptide + unmodified peptide) × 100%; OH, hydroxylation. *$P < 0.05$, diabetic vs. control ($n = 3$).

whether HOCl can cause oxidation and chlorination of specific tryptophan residues, NC1 hexamers isolated from nondiabetic control rat kidneys were treated with different concentrations of HOCl (Fig. 4). This treatment resulted in specific modification of the same W^{192} residue of α1NC1 domain as in the samples isolated from diabetic kidneys. The levels of either oxidized or chlorinated W^{192} residue were proportional to HOCl concentration, and at 0.2 mmol/L HOCl the levels of both modifications were similar to those found in diabetic kidneys (Fig. 4 and Table 2). HOCl treatment also caused similar oxidation and chlorination of W^{28} of the α2NC1 domain (data not shown).

MD Simulations

To predict the impact of oxidation and chlorination of W^{28} and W^{192} residues on NC1 hexamer structure, we performed MD simulations. Molecular modeling showed that residue W^{28} is located on β-strand 2 of the α2 monomer, forming a hydrophobic surface along an interface with the adjacent α1 monomer (Fig. 5*A* and *B*). Residue W^{192} is located on β-strand 8 of α1 monomer and adjacent to the β-hairpin domain swapping region that is essential for monomer association and subsequent hexamer assembly (34,35) (Fig. 5*A* and *C*).

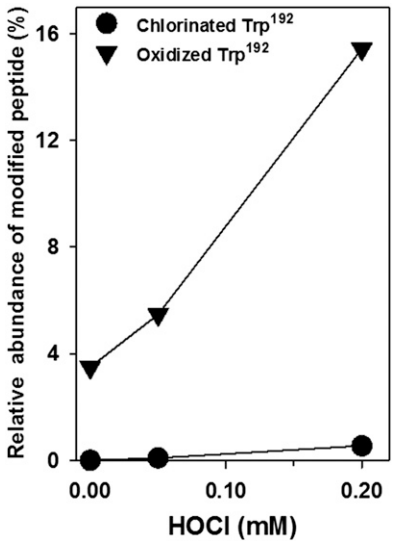

Figure 4—Effect of HOCl treatment on chlorination and oxidation of W^{192} of the α1NC1 domain within NC1 hexamer of collagen IV isolated from rat kidneys. Isolated NC1 hexamers were incubated in 50 mmol/L TBS, pH 7.4, for 2 h at 37°C alone or with the indicated concentrations of HOCl. Samples were analyzed using LC-MS/MS, as described in RESEARCH DESIGN AND METHODS.

Global structural properties were extracted from the MD trajectories for comparison. Comparison of NC1 $(\alpha1,\alpha1,\alpha2)_2$ hexamer radii of gyration indicate that both chlorinated and oxidized structures induce an increase in the hexamer radius of ~0.3 Å relative to the control structure (Fig. 5*D*). Measurement of the solvent-accessible surface area of the hexamer indicated an increase of ~4,000 $Å^2$ for both oxidized and chlorinated systems (Fig. 5*E*). Radial distribution functions were calculated for W^{28} and W^{192} of each NC1 α-chain relative to protein or water atoms and compared between control and modified systems. There was a lower probability of observing NC1 domain atoms within a distance of 3–15 Å from the center of mass of W^{28} residue for either the oxidized or the chlorinated MD system compared with the control (Fig. 5*F*). The inverse effect was observed for solvent water atoms (Fig. 5*G*). These results are consistent with a less compact fold of either oxidized or chlorinated NC1 hexamer compared with unmodified control hexamer.

Structural perturbations induced by either oxidized or chlorinated tryptophan residues were quantified by measurement of their root mean square deviation (RMSD) from an unmodified control (Fig. 5*H*, *I*, and inset table, and Supplementary Fig. 5). RMSD values of the modified tryptophan residues produced changes in the range of 7–9 Å in oxidized structures and 4–7 Å in chlorinated structures. Molecular modeling indicated that either oxidized or chlorinated W^{28} residues induced localized structural perturbations, resulting in composite RMSD values of about 27–28 Å to the β-sheet, comprised of β1, β2, and β10 strands (Fig. 5*H*, *I*, and inset table). Modification of W^{192} had a disruptive effect (RMSD 23–24 Å) on conformation of the β-hairpin insert comprised of β6′ and β7′ (Fig. 5*H*, *I*, and inset table). These results suggest that modification of W^{192} of α1NC1 and W^{28} of α2NC1 can

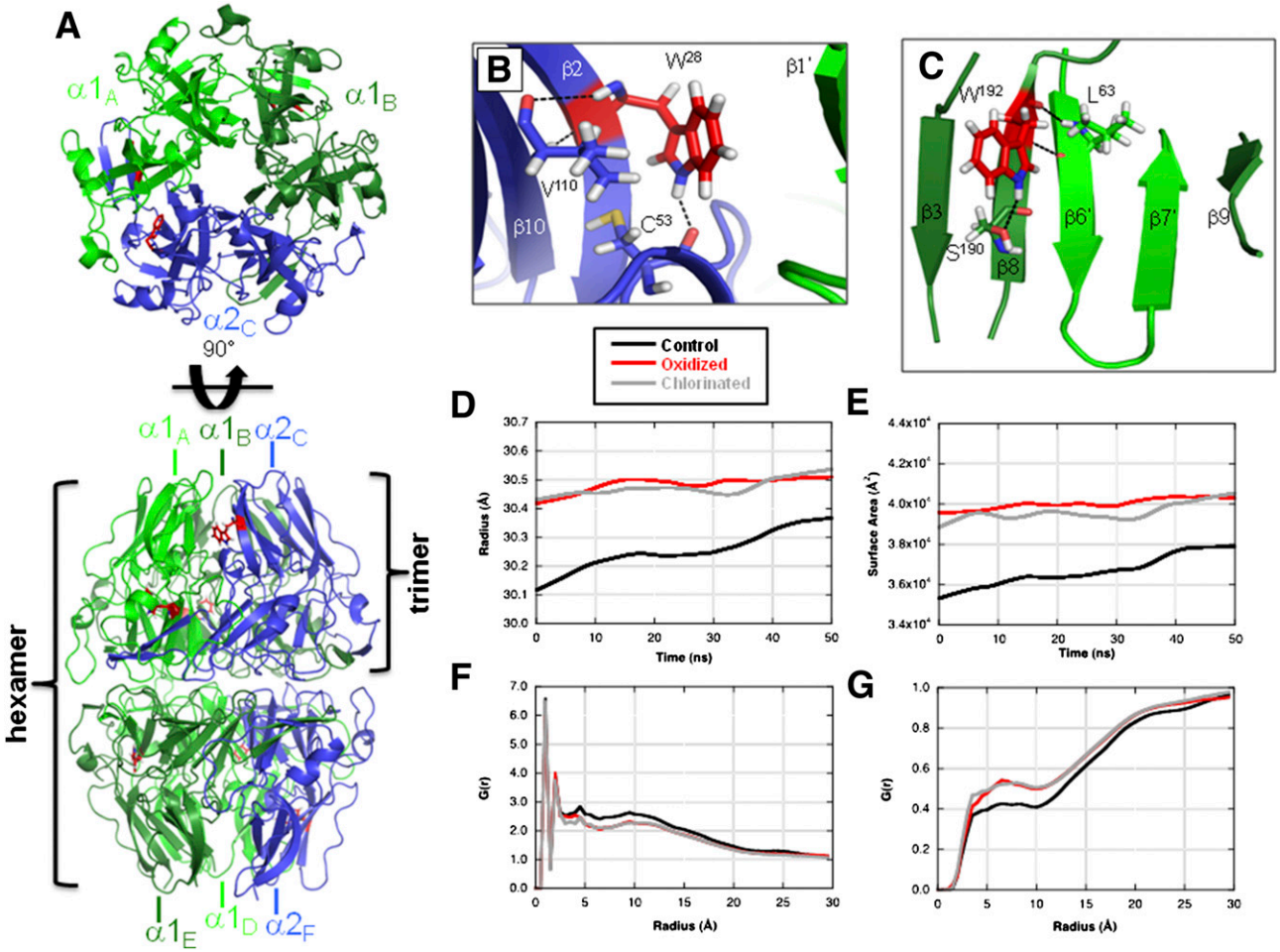

Figure 5—MD simulation model of the impact of oxidized/chlorinated tryptophan residues on the NC1 $(\alpha1,\alpha1,\alpha2)_2$ hexamer structure. *A*: MD simulations were conducted with one modified tryptophan per NC1 monomer. Locations of W^{28} (*B*) and W^{192} (*C*) residues are shown within NC1 hexamer. The radius of gyration (*D*) and solvent-accessible surface area (*E*) for an unmodified control hexamer (black), a hexamer oxidized at W^{28} and W^{192} (red), and a hexamer chlorinated at W^{28} and W^{192} (gray) are shown. The radial distribution function, *G*(*r*), is shown for α2 monomer relative to both solute atoms (*F*) and water molecules (*G*). Local conformational perturbations introduced by selected oxidized W^{28} and W^{192} NC1 hexamer residues are shown in panels *H* and *I*, respectively. Superimposed control (gray) and oxidized (green and blue) structures are shown with color scheme and subunit nomenclature corresponding to those in panel *A*. The average RMSD values for all W^{28} and W^{192} residues in modified relative to control NC1 hexamers are shown in the inset table. RMSD values were calculated for all atoms of either W^{28} or W^{192} residues or for backbone heavy atoms of the adjacent secondary structure elements. *J*: Limited proteolysis of HOCl-modified NC1 hexamer by proteinase K (PrK) was performed as described in RESEARCH DESIGN AND METHODS. A limited proteolysis experiment was performed three times with the same results. MW Std., molecular weight standard.

induce localized structural perturbations within domain swapping and domain interface regions that are critical for NC1 hexamer assembly and stability.

A less compact structure and a decrease in the stability of modified NC1 hexamer predicted by MD simulations were confirmed using a limited proteolysis approach. HOCl-modified NC1 hexamer was more susceptible to proteolysis by proteinase K compared with native hexamer (Fig. 5*J*).

Effect of HOCl-Derived Modifications on NC1 Domain Refolding and Hexamer Assembly

MD simulations predicted that HOCl-derived modifications can compromise local NC1 hexamer conformation at the domain interfaces. This may affect assembly competence, one of the key functional properties of NC1 domains. To validate this prediction, we investigated refolding of NC1 domains and hexamer assembly using denaturing solution conditions. NC1 hexamers isolated from control and diabetic rats were stable under non-denaturing solution conditions with <3% of the monomeric form present (Fig. 6*A*). When NC1 hexamers were denatured with 6 mol/L GdnCl and injected onto a gel-filtration column to allow for refolding and assembly, specimens isolated from control rats formed assembly-competent domains and eluted mainly as hexamers (Fig. 6*B*). In contrast, specimens isolated from diabetic rats showed a significant decrease in the hexamer peak with a corresponding increase in the dimer and monomer peaks (Fig. 6*B*).

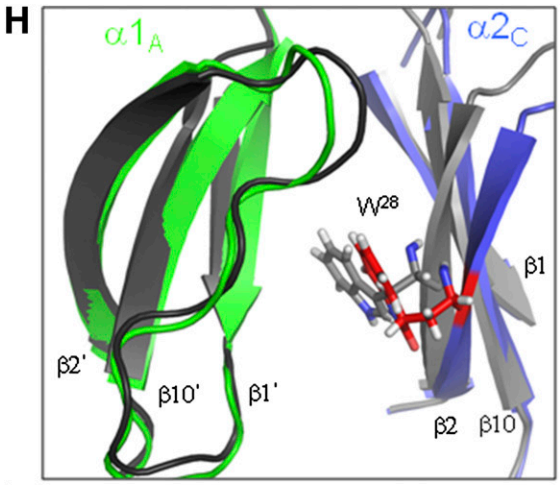

	Control	Oxidized	Chlorinated
		angstrom (Å)	
Residue W^{28}	-----	9.1±5.2	6.8±0.8
Strands β1, β2, β10	-----	28.1±0.6	27.2±1.4
Residue W^{192}	-----	7.3±2.1	4.3±1.2
Strands β6', β7'	-----	23.0±3.2	24.0±5.0

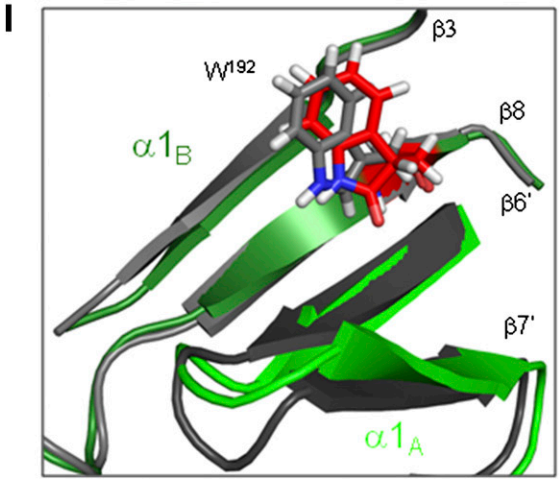

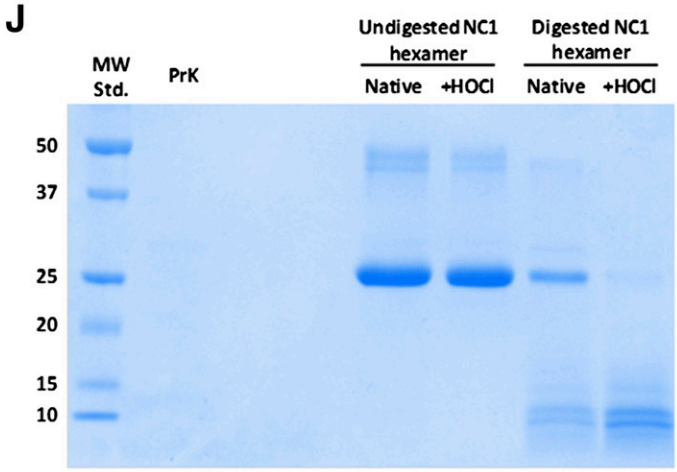

Figure 5—*Continued*.

Next, we determined whether the treatment of NC1 hexamers with HOCl can similarly affect hexamer refolding and assembly. Indeed, NC1 hexamers pretreated with the increasing concentrations of HOCl, followed by denaturation and refolding, progressively lost their ability to reassemble back to the hexameric state (Fig. 6*C*).

DISCUSSION

Nonenzymatic post-translational modifications (NPTMs) of proteins can contribute to epigenetic disease mechanisms in diabetes. More abundant in the diabetic milieu, which promotes oxidative and glycoxidative reactions, these pathogenic NPTMs must affect sites critical for protein functionality. In the current study, we investigated oxidative NPTM of collagen IV in diabetes. We detected a significant increase in the levels of renal tissue halogenation in a type 1 diabetic rat model and in a type 2 diabetic nephropathy mouse model compared with the corresponding nondiabetic control groups.

We further demonstrated that diabetic halogenation of either renal ECM or collagen IV had a functional impact (i.e., inhibition of ECM interaction with α1β1 integrin, a primary collagen IV receptor that may be involved in the modulation of diabetic glomerular injury) (36). This is most likely due to the reactivity of HOCl and/or HOBr toward tyrosine, phenylalanine, and arginine, residues that are present within integrin binding sites of the ECM proteins (37–39). Interestingly, the inhibition of integrin binding was demonstrated upon modification of collagen IV with glycoxidative advanced glycation end products (AGEs), which specifically targeted arginine residues within integrin binding sites (40–43).

In experimental diabetes, chlorination and oxidation of two specific tryptophan residues, W^{28} and W^{192}, were significantly increased in NC1 hexamer, a key connection module of collagen IV networks. Importantly, modification levels of NC1 tyrosine residues were unchanged in diabetes versus control models, whereas a majority of other potential oxidation and halogenation sites were not modified (Fig. 3). This observation is consistent with the notion that NPTMs occur in vivo only at relatively few protein sites with a favorable microenvironment, so-called "hot spots" (44). The combined abundance of oxidized and chlorinated W^{28} and W^{192} residues in NC1 domains of collagen IV in diabetes was about 20 mol%, with oxidized tryptophan being a major contributor. It is

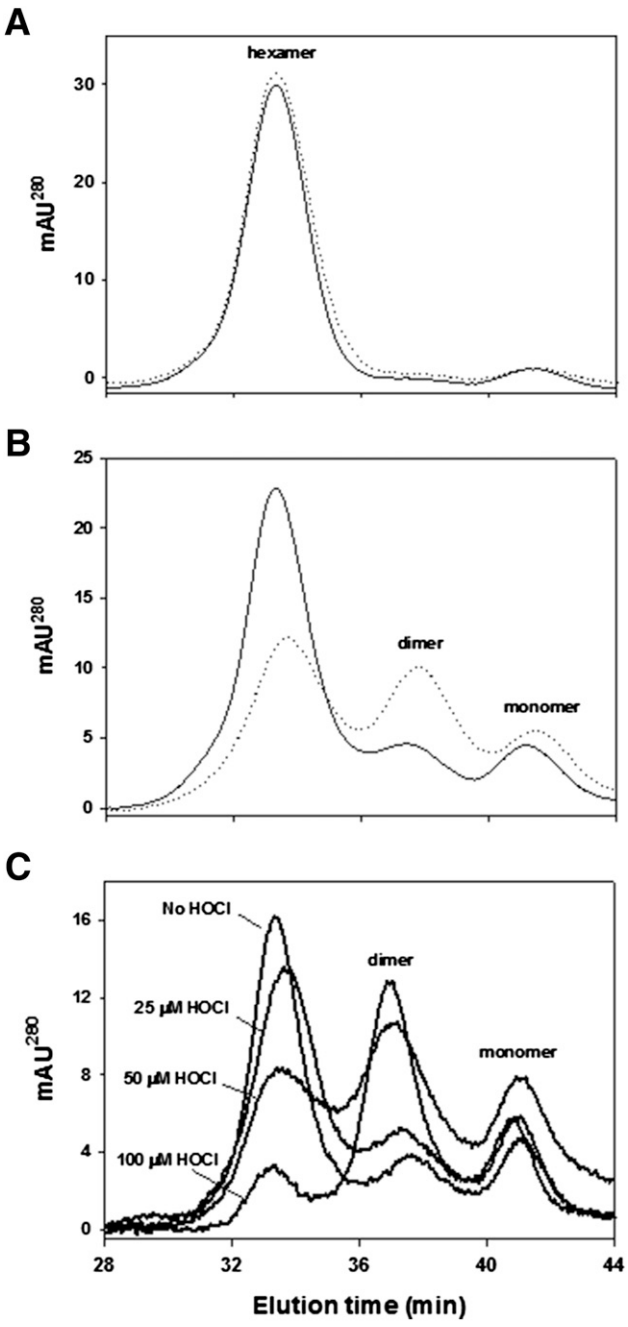

Figure 6—Refolding and assembly of diabetic and HOCl-modified NC1 hexamers of collagen IV. NC1 hexamers isolated from kidneys of control (solid line) and diabetic (dotted line) rats were incubated in 50 mmol/L Tris acetate buffer, pH 7.4, at 4°C (*A*) or in the same buffer supplemented with 6 mol/L GdnCl at 80°C for 30 min (*B*). Samples were injected onto an FPLC gel filtration column equilibrated with 50 mmol/L Tris acetate buffer to allow for NC1 domain refolding and hexamer assembly and were analyzed as described in RESEARCH DESIGN AND METHODS. *C*: Isolated rat renal NC1 hexamers were incubated in 50 mmol/L TBS, pH 7.4, or in the same buffer supplemented with the indicated concentrations of HOCl for 2 h at 37°C. The final protein concentration was 0.2 mg/mL. Samples were then supplemented with 6 mol/L GdnCl and incubated at 80°C for 30 min. Samples were injected onto a gel filtration FPLC column and analyzed as in *A* and *B*. AU, absorbance unit.

noteworthy that these abundance levels are comparable to the levels of many common AGEs found in ECM proteins in vivo (45).

Although the levels of chlorotryptophan in diabetic NC1 domain were relatively low compared with tryptophan oxidation, this is the first report of chlorinated tryptophan residues in a protein. Increased levels of chlorotyrosine have been previously detected in LDL and HDL in atherosclerotic lesions (46,47). We did not detect chlorotyrosine in NC1 domains of collagen IV, possibly because the tryptophan side chain is ~1,000-fold more reactive with HOCl than the side chain of tyrosine (37). Thus, tyrosine chlorination may be disfavored in the presence of highly reactive tryptophan residues within NC1 hexamer. In diabetes, other oxidative modifications of tryptophan and tyrosine residues have been found (e.g., hydroxytryptophan [48], dityrosine [49], and nitrotyrosine [50,51]). The novel chlorotryptophan modification, identified in both animal and human collagen IV (Supplementary Table 1 and Supplementary Fig. 4), points to a potential pathogenic role of HOCl in diabetes and diabetes complications. Compared with chlorotryptophan, oxidized tryptophan was a major modification of collagen IV NC1 domain in diabetes and can also be a product of reaction with HOCl (37). In fact, HOCl reactivity may be a major source of oxidized tryptophan, since NC1 hexamers treated in vitro with HOCl produced the same relative levels of chlorinated and oxidized tryptophan residues as those isolated from diabetic kidneys (Table 2 and Fig. 4). We also found bromotyrosine, a modification that has not been previously reported in renal tissues in vivo. A single bromination site was located at Y^6 within the N-terminal region of the α2NC1 domain adjacent to the collagenous domain (Fig. 3). However, the level of bromination at this site did not change in animals with diabetes compared with controls.

The potential source of damaging hypohalous acids can be peroxidase enzymes, such as MPO and peroxidasin (2,3). These enzymes can produce both HOCl and HOBr (9–11), and have been shown to bind to ECM (3,8,16). Although they carry out important homeostatic functions in normal physiology, it is possible that in disease models MPO and peroxidasin can cause off-target damage to long-lived ECM proteins.

Oxidized and chlorinated W^{192} and W^{28} residues are located within critical regions at subunit interfaces of NC1 hexamers, and caused a disruption of local and global hexamer structures, a decrease in hexamer stability, and an increase in susceptibility to proteolytic degradation. Thus, contrary to a widely accepted paradigm, diabetic ECM may not necessarily be uniformly rigid and resistant to proteolysis due to excessive AGE cross-linking (45). Some ECM regions such as NC1 connecting points of collagen IV networks may be more susceptible to dissociation and/or degradation in diabetes.

In summary, we demonstrated hypohalous acid–induced functional damage to renal collagen IV networks and

their hexameric NC1 connection modules in diabetes. Our results suggest that modification of collagen IV by hypohalous acids in diabetes can decrease collagen IV network stability, increase its susceptibility to proteolysis, and inhibit its interaction with renal cells. Therefore, diabetic ECM modifications derived from hypohalous acids can potentially contribute to several pathologic phenomena observed in diabetic kidney disease, as follows: *1*) the increased porosity of renal ECM (52), *2*) podocyte detachment from the glomerular basement membrane and podocyturia (53,54), and *3*) the exacerbation of renal pathology due to the loss of cell-collagen IV interactions mediated by α1β1 integrin (36). It follows that the protection of ECM from damage by hypohalous acids in diabetes has therapeutic potential.

Acknowledgments. The authors thank Ms. Parvin Todd, Vanderbilt University, for expert technical help, and Dr. Vadim Pedchenko, Vanderbilt University, for helpful discussions. The authors also thank the Vanderbilt Center for Structural Biology for the generous use of their computational facilities.

Funding. This work was supported by grants DK-65138 and DK-18381 from the National Institutes of Health (NIH). K.L.B. was supported by NIH grant 5T-32HL-94296-06. C.D. was supported by NIH research fellowship award T32-DK-007569-24S. H.M. was supported by NIH research fellowship grant DK-65123. J.A. and N.B. were supported by the Vanderbilt Aspirnaut program.

Duality of Interest. No potential conflicts of interest relevant to this article were reported.

Author Contributions. K.L.B., C.D., K.L.R., M.-Z.Z., and P.V. researched the data and wrote the manuscript. O.A.S., H.M., J.A., and N.B. researched the data and contributed to the discussion. A.F., R.H., and B.G.H. contributed to the discussion and reviewed and edited the manuscript. P.V. is the guarantor of this work and, as such, had full access to all the data in the study and takes responsibility for the integrity of the data and the accuracy of the data analysis.

References

1. Baynes JW, Thorpe SR. Role of oxidative stress in diabetic complications: a new perspective on an old paradigm. Diabetes 1999;48:1–9
2. Malle E, Buch T, Grone HJ. Myeloperoxidase in kidney disease. Kidney Int 2003;64:1956–1967
3. Bhave G, Cummings CF, Vanacore RM, et al. Peroxidasin forms sulfilimine chemical bonds using hypohalous acids in tissue genesis. Nat Chem Biol 2012;8:784–790
4. Zhang C, Yang J, Jennings LK. Leukocyte-derived myeloperoxidase amplifies high-glucose–induced endothelial dysfunction through interaction with high-glucose–stimulated, vascular non–leukocyte-derived reactive oxygen species. Diabetes 2004;53:2950–2959
5. Bai YP, Hu CP, Yuan Q, et al. Role of VPO1, a newly identified heme-containing peroxidase, in ox-LDL induced endothelial cell apoptosis. Free Radic Biol Med 2011;51:1492–1500
6. Shi R, Hu C, Yuan Q, et al. Involvement of vascular peroxidase 1 in angiotensin II-induced vascular smooth muscle cell proliferation. Cardiovasc Res 2011;91:27–36
7. Brandes RP. Vascular peroxidase 1/peroxidasin: a complex protein with a simple function? Cardiovasc Res 2011;91:1–2
8. Péterfi Z, Donkó A, Orient A, et al. Peroxidasin is secreted and incorporated into the extracellular matrix of myofibroblasts and fibrotic kidney. Am J Pathol 2009;175:725–735
9. Senthilmohan R, Kettle AJ. Bromination and chlorination reactions of myeloperoxidase at physiological concentrations of bromide and chloride. Arch Biochem Biophys 2006;445:235–244
10. Wu W, Chen Y, d'Avignon A, Hazen SL. 3-Bromotyrosine and 3,5-dibromotyrosine are major products of protein oxidation by eosinophil peroxidase: potential markers for eosinophil-dependent tissue injury in vivo. Biochemistry 1999;38:3538–3548
11. McCall AS, Cummings CF, Bhave G, Vanacore R, Page-McCaw A, Hudson BG. Bromine is an essential trace element for assembly of collagen IV scaffolds in tissue development and architecture. Cell 2014;157:1380–1392
12. Liu B, Hou X, Zhou Q, et al. Detection of advanced oxidation protein products in patients with chronic kidney disease by a novel monoclonal antibody. Free Radic Res 2011;45:662–671
13. Xu J, Xie Z, Reece R, Pimental D, Zou MH. Uncoupling of endothelial nitric oxidase synthase by hypochlorous acid: role of NAD(P)H oxidase-derived superoxide and peroxynitrite. Arterioscler Thromb Vasc Biol 2006;26:2688–2695
14. Yang J, Ji R, Cheng Y, Sun JZ, Jennings LK, Zhang C. L-arginine chlorination results in the formation of a nonselective nitric-oxide synthase inhibitor. J Pharmacol Exp Ther 2006;318:1044–1049
15. Nicholls SJ, Zheng L, Hazen SL. Formation of dysfunctional high-density lipoprotein by myeloperoxidase. Trends Cardiovasc Med 2005;15:212–219
16. Kubala L, Kolářová H, Viteček J, et al. The potentiation of myeloperoxidase activity by the glycosaminoglycan-dependent binding of myeloperoxidase to proteins of the extracellular matrix. Biochim Biophys Acta 2013;1830:4524–4536
17. Hudson BG, Tryggvason K, Sundaramoorthy M, Neilson EG. Alport's syndrome, Goodpasture's syndrome, and type IV collagen. N Engl J Med 2003;348:2543–2556
18. Zhao HJ, Wang S, Cheng H, et al. Endothelial nitric oxide synthase deficiency produces accelerated nephropathy in diabetic mice. J Am Soc Nephrol 2006;17:2664–2669
19. Kanetsuna Y, Takahashi K, Nagata M, et al. Deficiency of endothelial nitric-oxide synthase confers susceptibility to diabetic nephropathy in nephropathy-resistant inbred mice. Am J Pathol 2007;170:1473–1484
20. Kato Y, Kawai Y, Morinaga H, et al. Immunogenicity of a brominated protein and successive establishment of a monoclonal antibody to dihalogenated tyrosine. Free Radic Biol Med 2005;38:24–31
21. Zhang MZ, Yao B, Cheng HF, Wang SW, Inagami T, Harris RC. Renal cortical cyclooxygenase 2 expression is differentially regulated by angiotensin II AT(1) and AT(2) receptors. Proc Natl Acad Sci U S A 2006;103:16045–16050
22. Kahsai TZ, Enders GC, Gunwar S, et al. Seminiferous tubule basement membrane. Composition and organization of type IV collagen chains, and the linkage of alpha3(IV) and alpha5(IV) chains. J Biol Chem 1997;272:17023–17032
23. Pedchenko V, Zent R, Hudson BG. Alpha(v)beta3 and alpha(v)beta5 integrins bind both the proximal RGD site and non-RGD motifs within noncollagenous (NC1) domain of the alpha3 chain of type IV collagen: implication for the mechanism of endothelia cell adhesion. J Biol Chem 2004;279:2772–2780
24. Steinitz M, Baraz L. A rapid method for estimating the binding of ligands to ELISA microwells. J Immunol Methods 2000;238:143–150
25. Eng JK, McCormack AL, Yates JR. An approach to correlate tandem mass spectral data of peptides with amino acid sequences in a protein database. J Am Soc Mass Spectrom 1994;5:976–989
26. Voziyan P, Brown KL, Chetyrkin S, Hudson B. Site-specific AGE modifications in the extracellular matrix: a role for glyoxal in protein damage in diabetes. Clin Chem Lab Med 2014;52:39–45
27. Joung IS, Cheatham TE 3rd. Determination of alkali and halide monovalent ion parameters for use in explicitly solvated biomolecular simulations. J Phys Chem B 2008;112:9020–9041
28. Wu XW, Brooks BR. Self-guided Langevin dynamics simulation method. Chem Phys Lett 2003;381:512–518
29. Essmann U, Perera L, Berkowitz ML, Darden T, Lee H, Pedersen LG. A smooth particle mesh Ewald method. J Chem Phys 1995;103:8577–8593
30. *The PyMOL Molecular Graphics System*. Version 1.5.0.4. New York, Schrodinger, 2012
31. Vanacore R, Ham AJ, Voehler M, et al. A sulfilimine bond identified in collagen IV. Science 2009;325:1230–1234

32. Taylor SW, Fahy E, Murray J, Capaldi RA, Ghosh SS. Oxidative post-translational modification of tryptophan residues in cardiac mitochondrial proteins. J Biol Chem 2003;278:19587–19590
33. Szuchman-Sapir AJ, Pattison DI, Ellis NA, Hawkins CL, Davies MJ, Witting PK. Hypochlorous acid oxidizes methionine and tryptophan residues in myoglobin. Free Radic Biol Med 2008;45:789–798
34. Khoshnoodi J, Cartailler JP, Alvares K, Veis A, Hudson BG. Molecular recognition in the assembly of collagens: terminal noncollagenous domains are key recognition modules in the formation of triple helical protomers. J Biol Chem 2006;281:38117–38121
35. Sundaramoorthy M, Meiyappan M, Todd P, Hudson BG. Crystal structure of NC1 domains. Structural basis for type IV collagen assembly in basement membranes. J Biol Chem 2002;277:31142–31153
36. Zent R, Yan X, Su Y, et al. Glomerular injury is exacerbated in diabetic integrin alpha1-null mice. Kidney Int 2006;70:460–470
37. Pattison DI, Davies MJ. Absolute rate constants for the reaction of hypochlorous acid with protein side chains and peptide bonds. Chem Res Toxicol 2001;14:1453–1464
38. Bergt C, Oettl K, Keller W, et al. Reagent or myeloperoxidase-generated hypochlorite affects discrete regions in lipid-free and lipid-associated human apolipoprotein A-I. Biochem J 2000;346:345–354
39. Pattison DI, Davies MJ. Kinetic analysis of the reactions of hypobromous acid with protein components: implications for cellular damage and use of 3-bromotyrosine as a marker of oxidative stress. Biochemistry 2004;43:4799–4809
40. Pedchenko VK, Chetyrkin SV, Chuang P, et al. Mechanism of perturbation of integrin-mediated cell-matrix interactions by reactive carbonyl compounds and its implication for pathogenesis of diabetic nephropathy. Diabetes 2005;54:2952–2960
41. Pozzi A, Zent R, Chetyrkin S, et al. Modification of collagen IV by glucose or methylglyoxal alters distinct mesangial cell functions. J Am Soc Nephrol 2009;20:2119–2125
42. Chetyrkin S, Mathis M, Pedchenko V, et al. Glucose autoxidation induces functional damage to proteins via modification of critical arginine residues. Biochemistry 2011;50:6102–6112
43. Dobler D, Ahmed N, Song L, Eboigbodin KE, Thornalley PJ. Increased dicarbonyl metabolism in endothelial cells in hyperglycemia induces anoikis and impairs angiogenesis by RGD and GFOGER motif modification. Diabetes 2006;55:1961–1969
44. Thornalley PJ, Rabbani N. Protein damage in diabetes and uremia—identifying hotspots of proteome damage where minimal modification is amplified to marked pathophysiological effect. Free Radic Res 2011;45:89–100
45. Monnier VM, Mustata GT, Biemel KL, et al. Cross-linking of the extracellular matrix by the maillard reaction in aging and diabetes: an update on "a puzzle nearing resolution". Ann N Y Acad Sci 2005;1043:533–544
46. Hazen SL, Heinecke JW. 3-Chlorotyrosine, a specific marker of myeloperoxidase-catalyzed oxidation, is markedly elevated in low density lipoprotein isolated from human atherosclerotic intima. J Clin Invest 1997;99:2075–2081
47. Shao B, Pennathur S, Heinecke JW. Myeloperoxidase targets apolipoprotein A-I, the major high density lipoprotein protein, for site-specific oxidation in human atherosclerotic lesions. J Biol Chem 2012;287:6375–6386
48. Hamblin M, Friedman DB, Hill S, Caprioli RM, Smith HM, Hill MF. Alterations in the diabetic myocardial proteome coupled with increased myocardial oxidative stress underlies diabetic cardiomyopathy. J Mol Cell Cardiol 2007;42:884–895
49. Ueno Y, Horio F, Uchida K, et al. Increase in oxidative stress in kidneys of diabetic Akita mice. Biosci Biotechnol Biochem 2002;66:869–872
50. Hermo R, Mier C, Mazzotta M, Tsuji M, Kimura S, Gugliucci A. Circulating levels of nitrated apolipoprotein A-I are increased in type 2 diabetic patients. Clin Chem Lab Med 2005;43:601–606
51. Ahmed N, Babaei-Jadidi R, Howell SK, Beisswenger PJ, Thornalley PJ. Degradation products of proteins damaged by glycation, oxidation and nitration in clinical type 1 diabetes. Diabetologia 2005;48:1590–1603
52. Makino H, Shikata K, Hironaka K, et al. Ultrastructure of nonenzymatically glycated mesangial matrix in diabetic nephropathy. Kidney Int 1995;48:517–526
53. Petermann AT, Pippin J, Krofft R, et al. Viable podocytes detach in experimental diabetic nephropathy: potential mechanism underlying glomerulosclerosis. Nephron, Exp Nephrol 2004;98:e114–e123
54. Nakamura T, Ushiyama C, Suzuki S, et al. Urinary excretion of podocytes in patients with diabetic nephropathy. Nephrol Dial Transplant 2000;15:1379–1383